ISSN 0915-633X

NATIONAL INSTITUTE FOR FUSION SCIENCE

Exactly Conservative Semi-Lagrangian Scheme (CIP-CSL)
in One-Dimension

R. Tanaka, T. Nakamura and T. Yabe

(Received - Dec. 9, 1999)

NIFS-685 Feb. 2001

RESEARCH REPORT
NIFS Series

TOKI, JAPAN

Exactly Conservative Semi-Lagrangian Scheme (CIP-CSL) in One-Dimension

Ryotarou TANAKA, Takashi NAKAMURA and Takashi YABE

Department of Energy Sciences, Tokyo Institute of Technology,
Nagatsuta 4259, Yokohama 226-8502

Abstract

Two semi-Lagrangian schemes that guarantee exactly mass conservation are proposed. Although they are in a non-conservative form, the mass of each cell is employed as an additional variable that is advanced in a conservative form. One of them (CIP-CSL4) is the direct extension of the CIP method into the 4-th order polynomial to incorporate mass conservation. In another scheme (CIP-CSL2), the CIP principle is applied to integrated mass and the interpolation of the value becomes quadratic. The latter one can be readily extended to multi-dimensions. These schemes are applied to the non-linear advection problem with large CFL number.

Key Words : Semi-Lagrangian Schemes, Conservation, CIP, CFL,Berger's Equation

1 Introduction

Solving atmospheric problems together with oceanic ones and/or solid structure is a grand challenge to the field of computational mathematics. For these types of problems such as snow melting and deformation, and water evaporation , we need to treat topology and phase changes of the materials simultaneously, where the grid system aligned to the solid or liquid surface has no meaning and sometimes the mesh is distorted and even broken up. A universal treatment of all phases by one simple algorithm is thus essential and we are at the turning point of attacking this goal.

Even without phase change, problems of surface capturing and structure-fluid interaction are not easy task. In most of cases, the grid can not always be adapted to those surfaces. Therefore, the description of moving surfaces of complicated shape in the Cartesian grid system will be a challenging subject .

In order to attack the problems mentioned above, we must first find a method to treat a sharp interface and to solve the interaction of compressible gas with incompressible liquid or solid. Toward this goal, we take Eulerian-approach based on the CIP(cubic-interpolated propagation) method[1, 2, 3, 4] which does not need adaptive grid system and therefore removes the problems of grid distortion caused by structural break up and topology change. The material surface can be captured by almost one grid throughout the computation[5, 6, 7]. Furthermore, the scheme can treat all the phases of matter from solid state through liquid and two phase state to gas without restriction on the time step from high sound speed[8].

Pressure-based algorithm coupled with semi-Lagrangian approach like the CIP proved to be stable and robust in analyzing these subjects. The only disadvantage of this method was the lack of conservative property. Recent version of the CIP-CSL4[9] can overcome this difficulty and povide exactly conservative semi-Lagrangian scheme. Since these scheme do not use the cubic polynomial but use different orders of polynomial, we re-define the name of these CIP families as "Constrained Interpolation Profile" and still keep the abbreviation, CIP. This means that various constraints such as the time evolution of spatial gradient, that is used in the original CIP method, or spatially integrated conservative quantities can be used to construct the profile. In this paper, we shall give a brief review of the CIP method and then propose a method to incorporate the conservative property in semi-Lagrangian schemes.

2 Review of the CIP method

2.1 Numerical difficulty

Although the nature is in a continuous world, digitization process is unavoidable in order to be implemented in numerical simulations. Primary goal of numerical algorithm will be to retrieve the lost information inside the grid cell between these digitized points. Most

of numerical schemes proposed before, however, did not take care of real solution inside the grid cell and resolution has been limited to the grid size. The CIP method proposed by one of the authors tries to construct a solution inside the grid cell close enough to this real solution of the given equation with some constraints. We here explain its strategy by using an advection equation,

$$\frac{\partial f}{\partial t} + u\frac{\partial f}{\partial x} = 0. \tag{1}$$

When the velocity is constant, the solution of Eq.(1) gives a simple translational motion of wave with a velocity u. The initial profile (solid line of Fig.1(a)) moves like a dashed line in a continuous representation. At this time, the solution at grid points is denoted by circles and is the same as the exact solution. However, if we eliminate the dashed line as in Fig.1(b), then the information of the profile inside the grid cell has been lost and it is hard to imagine the original profile and it is natural to imagine a profile like that shown by solid line in (c). Thus, numerical diffusion arises when we construct the profile by the linear interpolation even with the exact solution as shown in Fig.1(c). This process is called the first-order upwind scheme. On the other hand, if we use quadratic polynomial for interpolation, it suffers from overshooting. This process is the Lax-Wendroff scheme or Leith scheme.

What made this solution worse ? It is because we neglect the behavior of the solution inside a grid cell and merely follow after the smoothness of the solution. From this experience, we understand that a method incorporating the real solution into the profile within a grid cell is quite an important subject. We propose to approximate the profile as shown below. Let us differentiate Eq.(1) with spatial variable x, then we get

$$\frac{\partial g}{\partial t} + u\frac{\partial g}{\partial x} = -\frac{\partial u}{\partial x}g, \tag{2}$$

where g stands for the spatial derivative of f, $\partial f/\partial x$. In the simplest case where the velocity u is constant, Eq.(2) coincides with Eq.(1) and represents the propagation of spatial derivative with a velocity u. By this equation, we can trace the time evolution of f and g on the basis of Eq.(1). If g could be predicted to propagate like that shown by the arrows in Fig.1(d), the profile after one step would be limited to a specific profile. It is easy to imagine that by this constraint, the solution becomes much closer to the initial profile that is the real solution. Most importantly, the solution thus created gives a profile consistent with Eq.(1) even inside the grid cell. Importance of this consistency will be demonstrated in the next section.

If both the values of f and g are given at two grid points, the profile between these points can be interpolated by cubic polynomial $F(x) = ax^3+bx^2+cx+d$. Thus, the profile at n+1 step is readily obtained by shifting the profile by $u\Delta t$ like $f^{n+1} = F(x - u\Delta t), g^{n+1} = dF(x - u\Delta t)/dx$.

$$\begin{aligned} a_i &= \frac{g_i + g_{iup}}{\Delta x_i^2} + \frac{2(f_i - f_{iup})}{\Delta x_i^3}, \\ b_i &= \frac{3(f_{iup} - f_i)}{\Delta x_i^2} - \frac{2g_i + g_{iup}}{\Delta x_i}, \\ \Delta x_i &= x_{iup} - x_i \\ iup &= i - \mathrm{sgn}(u_i) \end{aligned} \tag{3}$$

$$\begin{aligned} f_i^{n+1} &= a_i\xi_i^3 + b_i\xi_i^2 + g_i^n\xi_i + f_i^n, \\ g_i^{n+1} &= 3a_i\xi_i^2 + 2b_i\xi_i + g_i^n, \end{aligned} \tag{4}$$

where we define $\xi_i = -u_i\Delta t$ and $\mathrm{sgn}(u)$ stands for the sign of u. Figure 2(a) shows a profile after 1000 steps with this CIP method for the propagation of a square wave.

Although there exist various polynomial functions such as linear, quadratic Lagrange, cubic Lagrange, cubic spline and quintic Lagrange [10], all of these schemes (except those using the linear interpolation function) need at least three points in constructing interpolation approximations in one dimension. A more compact scheme by which one can construct interpolation function of high accuracy with less computational stencils is desired in many situations, such as the calculations of discontinuities or large gradients. Moreover, in a model with a limited computational domain, different approximations for the derivatives have to be used at the grid points close to boundaries; these approximations are usually of lower order than the approximations used deeper in the interior. Thus, a scheme which uses less stencils may be advantageous in treating computational boundaries since less boundary points need to be handled. Another attractive feature of reducing stencils may be the reduction in data transfer in parallel implementations on distributed memory architectures. In this sense, the CIP seems to be attractive since it uses only one cell for computation even in three-dimensions.

The CIP is completely different from conventional semi-Lagrangian methods regarding the computation of derivatives. In the latter methods, as mentioned above, the gradient is calculated based on the function values at neighboring grid points by either assuming the continuity of the quantity, the first and sometimes the second order derivatives of the quantity at the mesh boundaries [11] or using approximations based on local grid points [12]. By special treatment of the

first derivatives of the interpolation function, the CIP achieves a compact form that uses only one mesh cell to construct the interpolation profile and provides subcell resolution.

2.2 Phase error of CIP

It would be interesting to examine phase error of various schemes using the method proposed by Purnell[11] and Utsumi *et.al.*[13]. Figure 3 summarizes those results. As is well known, phase speed of conventional schemes departs from the exact one, that is shown by the solid line, around $k\Delta x = \pi/2$. Surprisingly, however, the CIP can reproduce the correct phase speed even up to $k\Delta x = \pi$. This is remarkable because $k\Delta x = \pi$ means that one wavelength is described by three grid points. Let us consider the case shown in Fig.4, where values of the three points are zero. Even in this case, one wave can exist as shown in the figure. The CIP gives correct spatial gradients, which are non-zero at these points, and therefore it recognize the existence of the wave inside the grid cell. Any code that uses only the information of the value, that is zero now, can not correctly recognize the wave even if higher order polynomial is employed.

The importance of Eq.(2), that predicts the propagation of gradients, can be clearly demonstrated in comparison with the cubic spline[11] and the PPM [14] both of which have the third-order accuracy. Although the cubic spline uses the same cubic polynomial as the CIP, it can not reproduce the result of the CIP, because the gradient of the spline is determined merely from smoothness requirement. As is easily recognized, such a constraint that is independent of the original equation will not help to retrieve the profile inside the grid cell.

2.3 Interface tracking

Treatment of interface that lies between materials of different properties remains a formidable challenge to the computation of multi-phase fluid dynamics. Eulerian methods have proven robust in simulating flows with interfaces of complex topology. Generally, Eulerian methods use color function to distinguish the regions where different materials fall in. To accurately reproduce the physical processes across the interface transition region, keeping the compact thickness of the interface is of great importance. The finite difference schemes constructed on an Eulerian grid, however, intrinsically produce numerical diffusions to the solution of advection equation by which the interface is predicted temporally. Thus, the direct implementation of finite difference schemes (even of high order) can not maintain the compactness of the interface.

Various kinds of methods have been developed so far to achieve a compact and correctly defined interface by introducing extra programming. Among those mostly used algorithms are the level set methods and the VOF(volume of fluid) methods for front capturing, and others for front tracking [15]. Level set method that was firstly proposed by Osher and Sethian[16] gets around the computation of interfacial discontinuity by evaluating the field in higher dimensions. The interface of interest is then recovered by taking a subset of the field. Practically, the interface is defined as the zero level set of a distance function from the interface.

In a VOF kind method on the other hand, the interface needs to be reconstructed based on the volume fraction of fluid. VOF methods are mainly classified as SLIC(simple line interface calculation)algorithm and PLIC(piecewise linear interface calculation) algorithm according to the interpolation function used to represent the interface. The SLIC[17] makes use of piecewise constant reconstruction and the interfaces are approximated by lines aligned with mesh coordinates. A significant progress in VOF method was made by Youngs as the PLIC algorithm[18]. Since then, some improvements on the reconstruction of the VOF interface have been reported[19] [20] [21]. The PLIC estimates the interface with a truly piecewise linear approximation that improves largely the geometrical faithfulness of the method.

A comparison of different methods for tracking interface can be found in[22]. It is evident that sophisticated methods such as particle method, PLIC method and level set method(with reinitialization)[23] are relatively computational expensive.

In [5] and [6], we devised an interface tracking technique which appears efficient, geometrically faithful and diffusionless. The method is a combination of the CIP advection solver and a tangent function transformation.

Consider impermeable material occupying closed area $\Omega(t)$, we identify it with color function or density function $\phi(x, y, z, t)$ by the following definition

$$\phi(x,y,z,t) = \begin{cases} 1, & (x,y,z) \in \Omega(t), \\ 0, & \text{otherwise.} \end{cases}$$

Suppose this material moves at the local speed, the color function evolves then according to the following advection equation

$$L[\phi] \equiv \frac{\partial \phi}{\partial t} + \mathbf{u} \cdot \nabla \phi = 0, \tag{5}$$

where $\mathbf{u}$ is the local velocity.

It is known that solving the above equation by finite difference schemes in an Eulerian representation will

produce numerical diffusion and tend to smear the initial sharpness of the interfaces. In our method, rather than the original variable ϕ itself, its transformation, say $T(\phi)$, is calculated by the CIP. We specify $T(\phi)$ to be a function of ϕ only then we have

$$L[T(\phi)] = \frac{dT}{d\phi} L[\phi] = 0, \tag{6}$$

which is correct only for linear operator L such as $L \equiv \partial/\partial t + \mathbf{u} \cdot \nabla$ in Eq.(5). Thus, the solution ϕ of $L[T(\phi)] = 0$, that is

$$\frac{\partial T(\phi)}{\partial t} + \mathbf{u} \cdot \nabla T(\phi) = 0, \tag{7}$$

satisfies the equation $L[\phi] = 0$ and all the algorithms proposed for ϕ (schemes for advection equation) can be used to $T(\phi)$. Hopefully, by the considerable simplicity, this kind of techniques would be very attractive for practical implementation. Furthermore, quite variety of functional transformation can be used to obtain desired properties of solutions. For example, logarithmic and exponential function pair can be used to describe a density change of several orders of magnitudes and to avoid negative values. We here use a transformation of a tangent function for $T(\phi)$, that is,

$$T(\phi) = \tan[(1-\epsilon)\pi(\phi - 1/2)], \tag{8}$$

$$\phi = \tan^{-1} T(\phi)/[(1-\epsilon)\pi] + 1/2, \tag{9}$$

where ϵ is a small positive constant. The factor $(1-\epsilon)$ makes us get around $-\infty$ for $\phi = 0$ and ∞ for $\phi = 1$ and enables us to tune for a desired steepness of the transition layer.

Although ϕ experiences a rapid change from 0 to 1 at the interface, $T(\phi)$ shows a quite regular behavior. Because most of the values of $T(\phi)$ are concentrated near $\phi = 0$ and 1, the function transformation improves locally the spatial resolution near the large gradients. Thus, the sharp discontinuity can be described quite easily. The transformation of this kind is effective only for the case where the value of ϕ is limited to a definite range throughout the calculation, like the color function defined before.

This method does not involve any interface construction procedure and is quite economical in computational complexity. It should be also notified that the presented method is more attractive in 3-D computation since the extension of the scheme to 3-D is straightforward.

Figure 2(b) shows a 1D square wave propagation computed by the CIP method together with the tangent transformation, which we call "digitizer". The initial sharpness is well preserved and the discontinuities are advected with a correct speed.

3 Toward Conservative Semi-Lagrangian Scheme

The CIP method treats the advection term separately from other terms in general hyperbolic equations. This enables us to use a large CFL number ($\equiv u\Delta t/\Delta x$) simply applying the procedure of Eq.(4) to the far-upstream grid cell from which the Lagrangian particle started to the present position of concern. Thus Eq.(4) is modified to be

$$\begin{aligned} f_i^{n+1} &= a_m < \xi >^3 + b_m < \xi >^2 + g_m^n < \xi > + f_m^n, \\ g_i^{n+1} &= 3a_m < \xi >^2 + 2b_m < \xi > + g_m^n, \end{aligned} \tag{10}$$

where m is the point determined by

$$\begin{aligned} x_m < x_p < x_{m+1}, \quad for \quad u \le 0 \\ x_{m-1} < x_p < x_m, \quad for \quad u > 0, \end{aligned}$$

and x_p is the particle position of upstream departure point calculated by

$$x_p = x_i + \int_{t+\Delta t}^{t} u dt. \tag{11}$$

This time integration is performed along the particle trajectory. Thus, $< \xi >$ is the distance between these two points :

$$< \xi >= x_p - x_m \tag{12}$$

It should be noticed that ξ is neither $-u\Delta t$ nor $\int_{t+\Delta t}^{t} u dt$. In Eq.(10), a_m, b_m are given by simply replacing i by m in Eq.(3).

Even in multi-dimensions, the strategy to find this upstream departure point is common to all other semi-Lagrangian schemes. Although the semi-Lagrangian algorithm can significantly reduce the computation time particularly in parallel computation, the loss of exact mass conservation stemming from the separate treatment of the advection term inhibited itself from long-term atmospheric and oceanic applications. In this section, we shall propose a method to recover this mass conservation in such semi-Lagrangian schemes.

3.1 CIP-CSL4[9]

We discuss at first how to compute conservation law such as

$$\frac{\partial f}{\partial t} + \frac{\partial (uf)}{\partial x} = 0. \tag{13}$$

As already seen, the CIP adopted additional constraint, that is spatial gradient, to represent the profile inside the grid cell. For being endowed with the conservative property, we here add another constraint as

$$\rho_{i-1/2}^n = \int_{x_{i-1}}^{x_i} f^n dx, \tag{14}$$

Therefore the spatial profile must be constructed to satisfy this additional constraint. If this could be realized, f would be advanced in the non-conservative form with exact conservation in a form of ρ which could be advanced maintaining mass conservation

Keeping this point in mind, then the ith function piece $F_i(x)$ must be determined so as to satisfy the following constraints:

$$\begin{cases} F_i(x_{i-1}) = f(x_{i-1}) \ , \quad F_i(x_i) = f(x_i) \\ \partial F_i(x_{i-1})/\partial x = g(x_{i-1}) \ , \quad \partial F_i(x_i)/\partial x = g(x_i) \\ \int_{x_{i-1}}^{x_i} F_i(x)dx = \rho_{i-1/2}. \end{cases} \tag{15}$$

In order to meet the above constraints, a fourth-order polynomial can be chosen as the interpolation function $F_i(x)$. Thus the time development of f and g is calculated simply by shifting the interpolation function $F_i(x)$ by $u\Delta t$ in the same way as Eq.(4) of the CIP method as follows;

$$f_i^* = F_i(x_i - u_i^n \Delta t) = a_i^n \xi_i^4 + b_i^n \xi_i^3 + c_i^n \xi_i^2 + g_i^n \xi_i + f_i^n, \tag{16}$$

$$g_i^* = \partial F_i(x_i - u_i^n \Delta t)/\partial x = 4a_i^n \xi_i^3 + 3b_i^n \xi_i^2 + 2c_i^n \xi_i + g_i^n, \tag{17}$$

where $\xi_i = -u_i^n \Delta t$, and

$$\begin{aligned} a_i^n &= [-5\{6(f_{iup} + f_i)\Delta x_i - (g_{iup} - g_i)\Delta x_i^2 \\ &\qquad +12sgn(u_i^n)\rho_{i-sgn(u_i^n)/2}\}]/2\Delta x_i^5, \\ b_i^n &= [4\{(7f_{iup} + 8f_i)\Delta x_i - (g_{iup} - (3/2)g_i)\Delta x_i^2 \\ &\qquad +15sgn(u_i^n)\rho_{i-sgn(u_i^n)/2}\}]/\Delta x_i^4, \\ c_i^n &= [-3\{(4(2f_{iup} + 3f_i)\Delta x_i - (g_{iup} - 3g_i)\Delta x_i^2 \\ &\qquad +20sgn(u_i^n)\rho_{i-sgn(u_i^n)/2}\}]/2\Delta x_i^3, \\ \Delta x_i &= x_{iup} - x_i, \\ iup &= i - sgn(u_i^n) \end{aligned} \tag{18}$$

The problem left for us is to calculate the time development of ρ. If we define the flux passing through x_{i-1} and x_i during $[t, t + \Delta t]$ as $\Delta\rho_{i-1}$ and $\Delta\rho_i$ respectively, the time development of ρ is calculated by

$$\rho_{i-1/2}^{n+1} = \rho_{i-1/2}^n + \Delta\rho_{i-1}^n - \Delta\rho_i^n. \tag{19}$$

With the aid of Fig.5, it is clear that $\Delta\rho_i^n$ is defined by

$$\begin{aligned} \Delta\rho_i^n &= \int_{x_i - u_i^n \Delta t}^{x_i} F_i^n(x)dx \\ &= -\left(\frac{a_i^n}{5}\xi_i^4 + \frac{b_i^n}{4}\xi_i^3 + \frac{c_i^n}{3}\xi_i^2 + \frac{g_i^n}{2}\xi_i + f_i^n\right)\xi_i. \end{aligned} \tag{20}$$

where each coefficient is equivalent to Eq.(18) at the time step n.

Therefore, the solution of Eq.(13) is given by Eqs.(16)~(20). The result of square wave propagation is shown in Fig.2(c). Extension to more general equations is similar to the CIP Method [3].

3.2 CIP-CSL2

The previous section gave a method to incorporate the mass conservation into semi-Lagrangian scheme by simply extending the CIP to 4-th order polynomial. Although the increase of the order of polynomial improved the accuracy of the solution, the extension to multi-dimensions may become expensive in computational cost. We here propose an alternative method keeping the polynomical be cubic. We shall use the same system of equation as Eqs.(13),(14).

In the CIP, the time evolution of f and $g = \partial f/\partial x$ is used as constraints to define a cubic polynomial, while in the CIP-CSL4, constraints are now $f, \partial f/\partial x$ and $\int f dx$ giving 4-th order polynomial. It would be intresting to find a way to apply the CIP to the integrated value of f instead of f itself. The motivation to employ this analogy stems from the following advection equation.

$$\frac{\partial D}{\partial t} + u\frac{\partial D}{\partial x} = 0. \tag{21}$$

Interestingly, if we take a spatial derivative of Eq.(21) and define $D' \equiv \partial D/\partial x$, we obtain a conservative-type equation

$$\frac{\partial D'}{\partial t} + \frac{\partial (uD')}{\partial x} = 0. \tag{22}$$

Since Eq.(22) is the same as Eq.(13), then we come to an idea to use $D' = f$ in Eq.(22) and $D = \int f \ dx$ in Eq.(21). This procedure is exactly the same as Eq.(1) by simply replacing f by $\int f \ dx$, together with Eq.(2) in which g is replaced by f. Thus all the CIP procedure can be used for a pair of $\int f dx$ and f instead of f and $\partial f/\partial x$

By this analogy, we shall introduce a function :

$$D_i(x) = \int_{x_i}^{x} f(x')dx'. \tag{23}$$

In view of Eq.(20), $D_i(x)$ is merely $-\Delta\rho_i^n$ if x is set to $x_i - u_i^n \Delta t$, therefore $D_i(x)$ represents the accumulated mass from x_i to the upstream point. We shall use a cubic polynomial to approximate this profile.

$$D_i(x) = A1_i X^3 + A2_i X^2 + f_i^n X \tag{24}$$

where $X = x - x_i$. The role of spatial gradient g in the CIP method is now played by f that is spatial gradient of $D(x)$ in the present scheme. By using the

above relation, a profile of $f(x)$ between x_i and x_{iup} is then given by taking the derivative of Eq.(24);

$$f(x) = \frac{\partial D_i(x)}{\partial x} = 3A1_i X^2 + 2A2_i X + f_i^n \qquad (25)$$

From the definition of D in Eq.(23), it is clear that

$$D_i(x_i) = 0, \qquad D_i(x_{iup}) = -\mathrm{sgn}(u_i)\rho^n_{icell} \quad (26)$$

where ρ^n_{icell} is the total mass of upwind cell defined at the cell center $i \pm 1/2$ and $icell = i - sgn(u_i)/2$. Since $\partial D/\partial x$ gives a functional value f, it is also clear that

$$\frac{\partial D_i(x_i)}{\partial x} = f_i^n, \qquad \frac{\partial D_i(x_{iup})}{\partial x} = f^n_{iup} \qquad (27)$$

Therefore, the coefficients $A1_i$ and $A2_i$ are determined so as to satisfy the constraints Eqs.(26) and (27). As a result of above simultaneous equations, the coefficients are determined explicitly without any matrix solution as follows ;

$$A1_i = \frac{f_i^n + f^n_{iup}}{\Delta x_i^2} + \frac{2\mathrm{sgn}(u_i)\rho^n_{icell}}{\Delta x_i^3} \qquad (28)$$

$$A2_i = -\frac{2f_i^n + f^n_{iup}}{\Delta x_i} - \frac{3\mathrm{sgn}(u_i)\rho^n_{icell}}{\Delta x_i^2} \qquad (29)$$

where $\Delta x_i \equiv x_{iup} - x_i$. Then, $\Delta\rho_i$ is calculated as,

$$\begin{aligned}\Delta\rho_i &= \int_{x_i+\xi}^{x_i} f(x')dx' = -D_i(x_i+\xi) \\ &= -(A1_i\xi^3 + A2_i\xi^2 + f_i^n\xi), \end{aligned} \qquad (30)$$

the time development of ρ can be calculated from Eq.(19) with the aid of Eq.(30). It is interesting to observe by comparing Eq.(28) with Eq.(3) that the role of f, g in Eq.(3) is played by D, f, respectively, because $D_i(x_i) - D_i(x_{iup}) = \mathrm{sgn}(u_i)\rho^n_{icell}$ from Eq.(26).

Then, let us turn to the time evolution of the physical value f. We calculate the physical value f in the same way as the original CIP scheme. Conservative equation is rewritten as

$$\partial f/\partial t + u\partial f/\partial x = G, \qquad (31)$$

where $G \equiv -f\partial u/\partial x$. Equation (31) is a simple advection equation for f. On the basis of the time-splitting algorithm of the CIP scheme [3], we split the solution of Eq. (31) into two phases;

$$advection\ phase: \qquad \partial f/\partial t + u\partial f/\partial x = 0 \qquad (32)$$

$$non-advection\ phase: \quad \partial f/\partial t = G \qquad (33)$$

After the advection phase is solved, the non-advection phase is calculated with the result of the advection phase.

In the advection phase, we make use of the local analytic solution of Eq.(32), that is well known as the Lagrangian invariant solution $f(x_i, t+\Delta t) = f(x_i - u_i\Delta t, t)$. Since the profile of $f(x)$ between x_i and x_{iup} is given by Eq.(25), the solution of the advection phase f^* is calculated as

$$f_i^* = \frac{\partial D_i(x_i+\xi)}{\partial x} = 3A1_i\xi^2 + 2A2_i\xi + f_i^n \qquad (34)$$

After the advection phase is calculated by using above Eq.(34), the result of the advection phase f^* is advanced to the value of the next time step f^{n+1} in the non-advection phase. The non-advection phase can be solved by conventional finite difference method as follows,

$$f_i^{n+1} = f_i^* + G\Delta t \qquad (35)$$

where $G = -f_i^*(\partial u/\partial x)_i$ and the spatial derivative of the velocity $\partial u/\partial x$ is approximated by the simple centered finite difference. Figure 2 (d) shows the result of the square wave propagation after 1000 time steps. We see from Fig.2, the CIP-CSL2 scheme provides quite similar result to one of the original CIP.

3.3 Generalization

It would be useful to summarize all the procedure here although the procedure is available in other references and was already given in the previous sections. The basic equations are now

$$\frac{\partial f}{\partial t} + u\frac{\partial f}{\partial x} = -f\frac{\partial u}{\partial x} + S \equiv G, \qquad (36)$$

$$\frac{\partial f'}{\partial t} + u\frac{\partial f'}{\partial x} = -u'f' + G' \qquad (37)$$

where G includes a part of mass flux $\partial(uf)/\partial x$ in Eq.(13) and/or various source terms like diffusion. These equations are split into two phases:

$$\begin{aligned} &(1)\mathrm{Advection\ phase} \\ &\frac{\partial f}{\partial t} + u\frac{\partial f}{\partial x} = 0, \\ &\frac{\partial f'}{\partial t} + u\frac{\partial f'}{\partial x} = 0 \end{aligned} \qquad (38)$$

$$\begin{aligned} &(2)\mathrm{Non-advection\ phase} \\ &\frac{\partial f}{\partial t} = G, \\ &\partial f'/\partial t = -u'f' + G' \end{aligned} \qquad (39)$$

The advection phase is solved by

$$\begin{aligned} &\mathrm{forCIP-CSL4} \\ &f_i^* = a_i^n\xi_i^4 + b_i^n\xi_i^3 + c_i^n\xi_i^2 + f_i'^n\xi_i + f_i^n, \\ &f_i'^* = 4a_i^n\xi_i^3 + 3b_i^n\xi_i^2 + 2c_i^n\xi_i + f_i'^n, \\ &\mathrm{forCIP-CSL2} \\ &f_i^* = 3A1_i\xi^2 + 2A2_i\xi + f_i^n \end{aligned}$$

The non-advection phase is written as

$$f_i^{n+1} = f_i^* + G\Delta t$$
$$f_i'^{n+1} = f_i'^* - (u_i'^* f_i'^*)\Delta t + \frac{f_{i+1}^{n+1} - f_{i+1}^* - f_{i-1}^{n+1} + f_{i-1}^*}{2\Delta x}, \quad (\mathrm{CIP-CSL4\ only})$$

For the calculation of $\rho\left(\equiv \int f\,dx\right)$, we use the conservative form of Eq.(36). Therefore it is solved as

$$\rho_{i-1/2}^* = \rho_{i-1/2}^n + \Delta\rho_{i-1}^n - \Delta\rho_i^n, \tag{40}$$

$$\rho_{i-1/2}^{n+1} = \rho_{i-1/2}^* + \int_{x_{i-1}}^{x_i} S dx \Delta t. \tag{41}$$

In the calculation of Eq.(40), Eq.(20) and Eq.(30) are used.

It is important to note that the mass conservation is recovered in a form of spatial profile within a grid cell every time step when the polynomial is re-constructed under the constraint of Eq.(14),even if mass flux is separately treated in the nonadvection term.

3.4 Numerical tests

We shall present some sample calculations to test the procedure given in the previous sections. The first example is advection with variable velocity and Eq.(13) is solved under a given velocity field;

$$u = 1 + 0.5\sin(2\pi x/100), \tag{42}$$

with the following initial condition,

$$f(0,x) = \begin{cases} 1 & if\ 40 \le x \le 60 \\ 0 & otherwise, \end{cases}$$

where equally spaced grid points of $\Delta x = 100/(N-1)$ and time step size of $\Delta t = 10/(N-1)$ are used, N being the number of grid points.

We repeated the calculation by changing the total grid points to N=101, 301 and 1001 to test grid dependence of the scheme proposed here and the results are shown in Fig.6. All profiles are those after $10(N-1)$ time steps that corresponds to t=100.

We confirm that the accuracy has been improved at the discontinuity by the CIP-CSL4 shceme, because it uses 4-th order polynomial and the CIP-CSL2 gives quite a similar result to the CIP. It is important to note that the first order upwind scheme needs 10,001 grid points to obtain the same result as the present schemes or the CIP of 101 grid points, which already converged to one solution regardless of grid size. Furthermore, it has already been shown that most of the modern schemes like TVD and ENO fail to reproduce the result with 101 grid points[24].

The following one-dimensional Burger's equation is an interesting example of application to non-linear equations.

$$\frac{\partial u}{\partial t} + u\frac{\partial u}{\partial x} = \lambda\frac{\partial^2 u}{\partial x^2} \equiv S. \tag{43}$$

Since the CIP and CIP-CSL4 need to calculate spatial derivative of u, we differentiate Eq.(43) as

$$\frac{\partial u'}{\partial t} + u\frac{\partial u'}{\partial x} = -u'^2 + S'. \tag{44}$$

The generalized procedure in the previous section is then applied to these equations.

For the calculation of $\rho\left(\equiv \int u\,dx\right)$, we transform Eq.(43) into the conservation form as follows,

$$\frac{\partial u}{\partial t} + \frac{\partial\left(u^2/2\right)}{\partial x} = S. \tag{45}$$

Therefore it is solved as

$$\rho_{i-1/2}^* = \rho_{i-1/2}^n + \Delta\rho_{i-1}^n - \Delta\rho_i^n, \tag{46}$$

$$\rho_{i-1/2}^{n+1} = \rho_{i-1/2}^* + \frac{\lambda\Delta t}{\Delta x^2}[\rho_{i+1/2}^* - 2\rho_{i-1/2}^* + \rho_{i-3/2}^*]. \tag{47}$$

We should note that in the calculation of Eq.(46), Eq.(20) and Eq.(30) are used but with $\xi = -u\Delta t/2$ must be used in view of convection velocity $u/2$ of Eq.(45). Finite difference approximation for viscous term is used in Eq.(47) since it is conservative.

Figure 7 shows the calculation result at t=100 with $\lambda = 0$ and the initial condition:

$$u\,(0,x) = 0.5 + 0.4\cos(2\pi x/100), \tag{48}$$

and equally spaced grid points of $\Delta x = 1.0$, time step size of $\Delta t = 0.1$, and mesh number $N = 101$ are used.

In order to check the exact speed of a shock wave, we show the result of the calculation by the first-order upwind scheme with N=1001 in the conservative form of Burger's equation .

In this calculation, although viscosity term is not included, the speed of a shock wave is exactly reproduced by the present schemes.

4 Semi-Lagrangian Calculation

As already stated, the CIP can be used for a large CFL number if the particle trajectory could be successfully traced according to Eq.(11) through variable velocity fields. Various methods have been proposed to find this trajectory [10, 25]. We shall use the 4-th order Runge-Kutta method for time integration of Eq.(11) although it is not necessary in one-dimension .

After the particle trajectory has been found, Eq.(10) is applied to advection phase. Most important procedure is to estimate the change of mass during such time interval. Let us imagine a procedure given in Fig.8. In this case, we must estimate how the mass develops according to Eqs.(19),(20). It would be complicated if we must compute the mass flux over the entire domain that the particle passes through. Fortunately, however, we can reduce this procedure with the help of Fig.8. Let us define the shaded regions by A, B and C, and then we can easily find that

$$\rho^n_{i-1/2} = A,$$
$$\Delta\rho^n_i = \int_{x_{m1}}^{x_i} F(x)dx = A + B,$$
$$\Delta\rho^n_{i-1} = \int_{x_{m2}}^{x_{i-1}} F(x)dx = B + C. \qquad (49)$$

Therefore, the new mass is simply given by

$$\rho^{n+1}_{i-1/2} = \rho^n_{i-1/2} + \Delta\rho^n_{i-1} - \Delta\rho^n_i = C = \int_{x_{m2}}^{x_{m1}} F(x)dx, \qquad (50)$$

which means the new mass is given by integrating the function value over the two grid points corresponding to the upstream departure points.

The target equation (13) contains two different parts ; one is advection that can be treated by the above-mentioned semi-Lagrangian procedure but another is the compression part like

$$\frac{\partial f}{\partial t} = -f\frac{\partial u}{\partial x}. \qquad (51)$$

The use of large time step sometimes leads to unstable solution owing to this term but usually it must be avoided because then the term should be solved accurately enough to realize physically reasonable solution. Thus, the use of large CFL number in Eq.(13) is allowed when the velocity variance Δu is quite small. This semi-Lagrangian approach is favorable when it is applied to the high-speed flow that could limit the time step but would not change the physical process even if large time step would be used. Therefore we should always keep in mind that the semi-Lagrangian scheme should be used under the limitation $\Delta u\Delta t/\Delta x < 1$, although the limitation from $u\Delta t/\Delta x < 1$ can be eliminated.

We apply the above procedure to the problem of variable velocity field of Eq.(42). Figure 9 shows some results containing various CFL numbers. Even up to CFL=5, the scheme works well.

5 Conclusion

We have proposed new algorithms that make non-conservative schemes be exactly conservative. In the mass conservation law, mass is used as an additional variable and it corrects the conservation error originated from a non-conservative formulation by continuously changing the shape of interpolation function. By this method, the total mass, which is defined to be the integrated value of f over the space, is exactly conserved.

This scheme has been tested by linear advection with variable velocity field and Burger's equation. Although further investigation would improve the result, the present scheme can provide a useful tool to solve nonlinear equation in a non- conservative representation which has been proven to be quite stable for multiphase flow calculations.

The extension to multi-dimensions may need a little concern about the introduction of integrated value of f and will be given in another paper appearing shortly.

Acknowledgement

This work was carried out under the collaborating research program at the National Institute for Fusion Science of Japan. We also thank Prof. F. Xiao at Tokyo Institute of Technology for careful reading of the manuscript and valuable suggestions.

REFERENCES

[1] H.Takewaki, A.Nishiguchi and T.Yabe , The cubic-interpolated pseudo-particle (CIP) method for solving hyperbolic-type equations, *J. Comput. Phys.* **61**, 261 (1985).

[2] H.Takewaki and T.Yabe , Cubic-interpolated pseudo particle (CIP) method - application to nonlinear or multi-dimensional problems-, *J.Comput.Phys.* **70** , 355 (1987).

[3] T.Yabe, and T. Aoki, A universal solver for hyperbolic-equations by cubic-polynomial interpolation. I. one-dimensional solver. *Comput. Phys. Commun.*, **66**, 219 (1991).

[4] T.Yabe, T. Ishikawa, P.Y.Wang, T.Aoki, Y.Kadota and F.Ikeda, A universal solver for hyperbolic-equations by cubic-polynomial interpolation. II. 2-dimensional and 3-dimensional solvers. *Comput. Phys. Commun.*, **66**, 233 (1991).

[5] T.Yabe and F.Xiao, Description of Complex and Sharp Interface during Shock Wave Interaction with Liquid Drop, *J. Phys. Soc. Japan* **62**, 2537(1993).

[6] T.Yabe and F.Xiao, Description of complex and sharp interface with fixed grids in incompressible and compressible fluid, *Computer Math. Applic.*, **29**, 15(1995).

[7] F.Xiao, T.Yabe, T.Ito and M.Tajima , An algorithm for simulating solid objects suspended

in stratified flow. *Comput Phys Commun.* **102**, 147 (1997).
[8] T.Yabe and P Y.Wang : Unified Numerical Procedure for Compressible and Incompressible Fluid, *J.Phys.Soc.Japan* **60** ,2105(1991).
[9] R.Tanaka,T.Nakamura and T.Yabe, Constructing exactly conservative scheme in a non-conservative form, *Comput. Phys. Commun.*,(1999) in press.
[10] A.Staniforth and J.Côté, Semi-Lagrangian integration scheme for atmospheric model-A review. *Mon. Wea. Rev.* , **119**, 2206 (1991).
[11] Purnell,D.K., Solution of the advective equation by upstream interpolation with a cubic spline *Mon. Wea. Rev.* . **104**, 42 (1975).
[12] D.L.Williamson, and P.J.Rasch, Two-dimensional semi-Lagrangian transport with shape-preserving interpolation. *Mon. Wea. Rev.* , **117**, 102 (1989).
[13] T.Utsumi, T.Kunugi, and T.Aoki, Stability and accuracy of the cubic interpolated propagation scheme, *Comput. Phys. Commun.*, **101**, 9 (1996).
[14] P.Colella and P.R.Woodward, The piecewise parabolic method (PPM) for gas-dynamical simulations,*J. Comput. Phys.*, **54**, 174(1984).
[15] S.O.Unverdi and G.A. Tryggvasson, A front-tracking method for viscous, incompressible, multi-fluid flows, *J. Comput. Phys.* **100**, 25(1992).
[16] S. Osher and J.A.Sethian, Front propagating with curvature-dependent speed: algorithms based on Hamilton-Jacobi formulations, *J. Comput. Phys.* **79**, 12(1988).
[17] C.W.Hirt and B.D.Nichols, Volume of fluid (VOF) method for the dynamics of free boundaries, *J. Comput. Phys.*, **39**, 201(1981).
[18] D.L.Youngs, Time-dependent multi-material flow with large fluid distortion, *Numer. Methods for Fluids Dynamics*, edited by K.W.Morton and M.J.Baines, p273 (1982).
[19] E.G.Puckett and J.S.Saltzman, A 3D adaptive mesh refinement algorithm for multimaterial gas dynamics, *Physica D* **60**, 84(1992).
[20] D.B. Kothe, W. J.Rider, S.J.Mosso, and J.S.Brock, Volume tracking of interface having surface tension in two and three dimension, AIAA paper 96-0859, 1996.
[21] E.G. Puckett, A.S. AlmgrenJ.B. Bell, D.L. Marcus and W. J.Rider, A high-order projection method for tracking fluid interfaces in variable density incompressible flows, *J. Comput. Phys.* **130**, 269 (1997).
[22] W.J.Rider and D.B.Kothe, Strentching and tearing interface tracking methods. *AIAA-95-1717* , 33th Aerospace Sciences Metting and Exhibit, Reno, NV, 1995.
[23] M. Sussman, P.Smereka and S.Osher, A level set approach for computing solutions to incompressible two-phase flow, *J. Comput. Phys.* **114**, 146(1994).
[24] R.Tanaka, T.Nakamura, T.Yabe and H.Wu , A class of conservative formulation of the CIP method, *CFD journal*,**8**, 1 (1999).
[25] P.K.Smolarkiewicz and J.A.Pudykiewicz, A class of semi-Lagrangian approximations for fluids, *J. Atomos. Sciences* ,**49**, 2082 (1992).

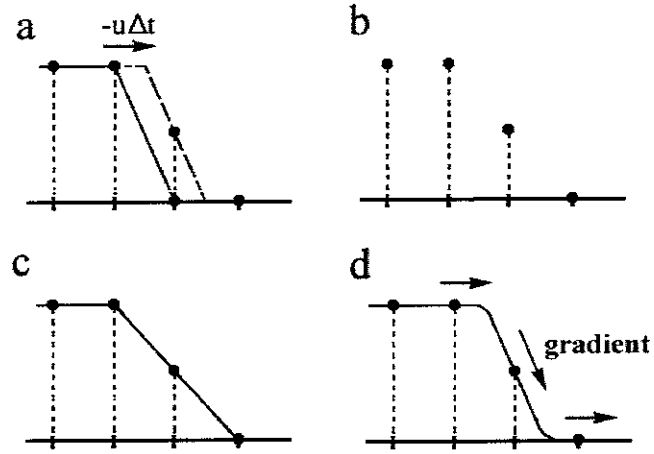

Fig.1 The principle of the CIP method. (a) solid line is initial profile and dashed line is an exact solution after advection, whose solution (b) at discretized points. (c) When (b) is linearly interpolated , numerical diffusion appears. (d) In the CIP, spatial derivative also propagates and the profile inside a grid cell is retrieved.

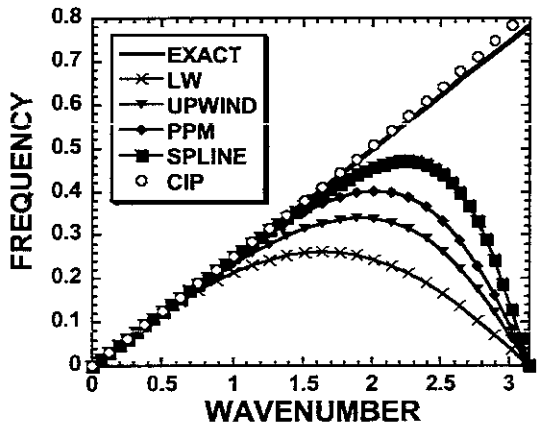

Fig.3 Phase error of various schemes such as 1st order upwind, Lax-Wendroff, PPM, Spline, and CIP.

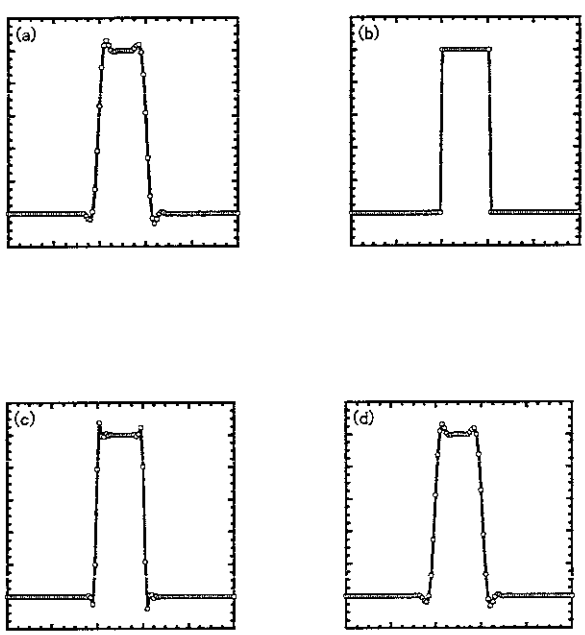

Fig.2 Square wave propagation with (a) CIP, (b) Digitized CIP, (c) CIP-CSL4 and (d) CIP-CSL2.

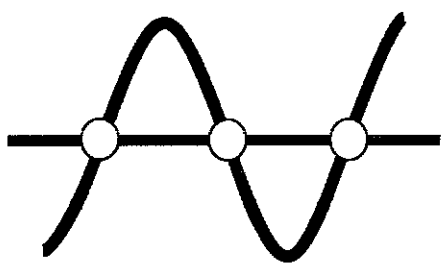

Fig.4 The CIP can correctly recognize one wavelength with three grids points.

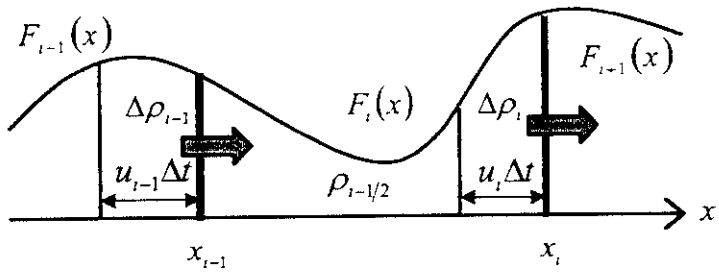

Fig.5 The inflow and outflow of flux during Δt.

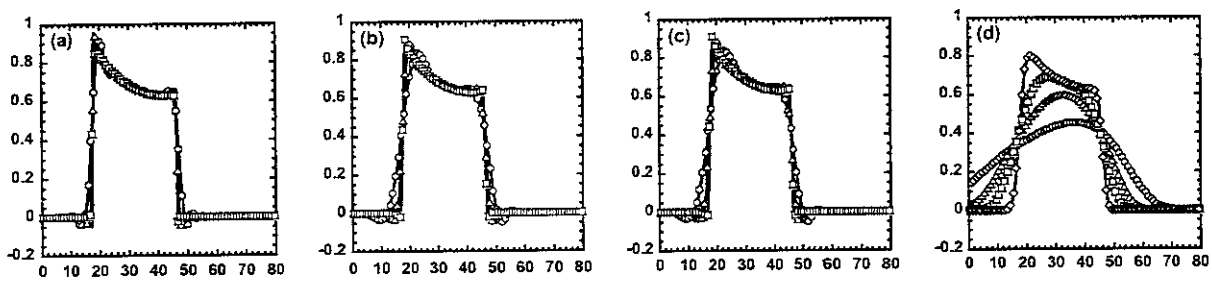

Fig.6 Propagation of a square wave with a given velocity field by (a) CIP-CSL4, (b) CIP-CSL2, (c) CIP and (d) the upwind scheme at t=100.
The number of grids is 101(circle), 301(triangle), 1001(square), 10001(diamond, only for upwind scheme).

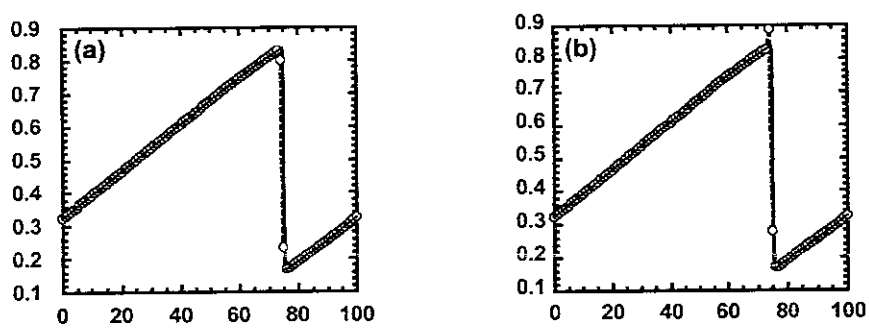

Fig.7 The result of Burger's equation without viscosity by (a) CIP-CSL4 and (b) CIP-CSL2 with 101 grid points at t=100. For comparison, the result of the first order upwind scheme with 1001 grid points at t=100 is shown by the solid line.

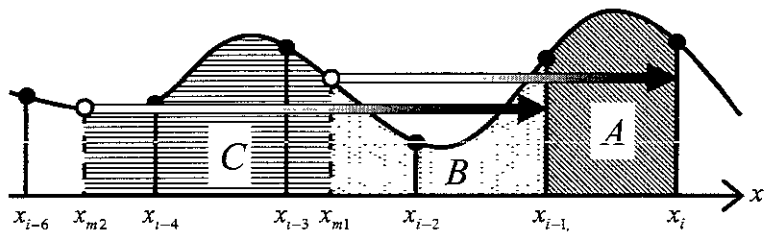

Fig.8 A method to evaluate the time evolution of mass flux.

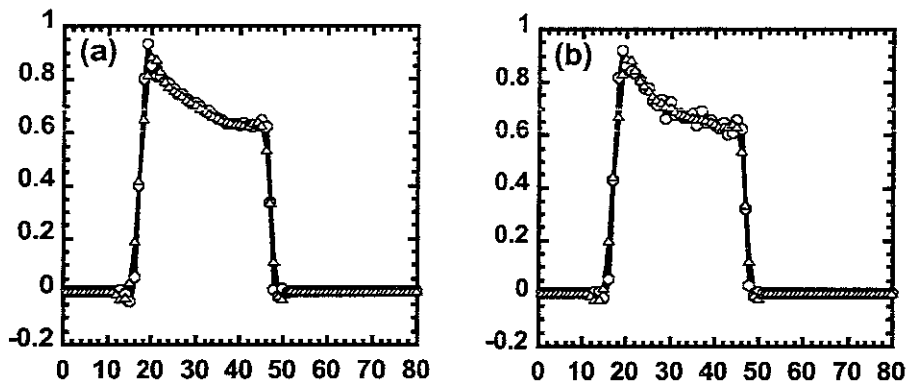

Fig.9 The same simulation as Fig.6 but with large CFL number, (a) CFL=2, (b) CFL=5, by CIP-CSL4(circle) and CIP-CSL2(triangle).

Recent Issues of NIFS Series

NIFS-662 T Hayashi, N Mizuguchi, H Miura and T Sato,
Dynamics of Relaxation Phenomena in Spherical Tokamak Sep 2000
(IAEA-CN-77THP2/13)

NIFS-663 H Nakamura and T Sato, H Kambe and K Sawada and T Saiki,
Design and Optimization of Tapered Structure of Near-field Fiber Probe Based on FDTD Simulation Oct 2000

NIFS-664 N Nakajima,
Three Dimensional Ideal MHD Stability Analysis in $L=2$ Heliotron Systems Oct 2000

NIFS-665 S Fujiwara and T Sato,
Structure Formation of a Single Polymer Chain I Growth of trans Domains Nov 2000

NIFS-666 S Kida,
Vortical Structure of Turbulence Nov 2000

NIFS-667 H. Nakamura, S Fujiwara and T Sato,
Rigidity of Orientationally Ordered Domains of Short Chain Molecules Nov 2000

NIFS-668 T Mutoh, R Kumazawa, T Seki, K Saito, Y Torii, F Shimpo, G Nomura, T Watari, D A Hartmann, M Yokota, K Akaishi, N Ashikawa, P deVries, M Emoto, H Funaba, M Goto, K Ida, H Idei, K Ikeda, S Inagaki, N Inoue, M Isobe, O Kaneko, K Kawahata, A Komori, T Kobuchi, S Kubo, S Masuzaki, T Morisaki, S Morita, J Miyazawa, S Murakami, T Minami, S Muto, Y Nagayama, Y Nakamura, H Nakanishi, K Narihara, N Noda, K Nishimura, K Ohkubo, N Ohyabu, S Ohdachi, Y Oka, M Osakabe, T Ozaki, B.J Peterson, A Sagara, N Sato, S Sakakibara, R Sakamoto, H Sasao, M Sasao, M Sato, T Shimozuma, M Shoji, S Sudo, H Suzuki, Y. Takeiri, K Tanaka, K Toi, T Tokuzawa, K Tsumori, K Y Watanabe, T Watanabe, H Yamada, I Yamada, S Yamaguchi, K Yamazaki, M Yokoyama, Y Yoshimura, Y. Hamada, O Motojima, M Fujiwara,
Fast- and Slow-Wave Heating of Ion Cyclotron Range of Frequencies in the Large Helical Device Nov 2000

NIFS-669 K Mima, M S Jovanovic, Y Sentoku, Z-M Sheng, M M Skoric and T Sato,
Stimulated Photon Cascade and Condensate in Relativistic Laser-plasma Interaction Nov 2000

NIFS-670 L Hadzievski, M M Skoric and T Sato,
On Origin and Dynamics of the Discrete NLS Equation Nov 2000

NIFS-671 K Ohkubo, S Kubo, H. Idei, T Shimozuma, Y Yoshimura, F Leuterer, M Sato and Y Takita,
Analysis of Oversized Sliding Waveguide by Mode Matching and Multi-Mode Network Theory Dec 2000

NIFS-672 C Das, S Kida and S Goto,
Overall Self-Similar Decay of Two-Dimensional Tirbulence Dec 2000

NIFS-673 L A Bureyeva, T Kato, VS Lisitsa and C. Namba,
Quasiclassical Representation of Autoionization Decay Rates in Parabolic Coordinates Dec 2000

NIFS-674 L A Bureyeva, VS. Lisitsa and C Namba,
Radiative Cascade Due to Dielectronic Recombination Dec 2000

NIFS-675 M.F Heyn, S V Kasilof, W Kernbichler, K Matsuoka, V V Nemov, S Okamura, O S Pavlichenko,
Configurational Effects on Low Collision Plasma Confinement in CHS Heliotron/Torsatron, Jan 2001

NIFS-676 K Itoh,
A Prospect at 11th International Toki Conference - Plasma physics, quo vadis?, Jan 2001

NIFS-677 S. Satake, H Sugama, M Okamoto and M Wakatani,
Classification of Particle Orbits near the Magnetic Axis in a Tokamak by Using Constants of Motion, Jan. 2001

NIFS-678 M. Tanaka and A Yu Grosberg,
Giant Charge Inversion of a Macroion Due to Multivalent Counterions and Monovalent Coions. Molecular Dynamics Studyn, Jan 2001

NIFS-679 K Akaishi, M Nakasuga, H Suzuki, M Iima, N Suzuki, A Komori, O Motojima and Vacuum Engineering Group,
Simulation by a Diffusion Model for the Variation of Hydrogen Pressure with Time between Hydrogen Discharge Shots in LHD, Feb 2001

NIFS-680 A Yoshizawa, N Yokoi, S Nisizima, S -I Itoh and K Itoh
Variational Approach to a Turbulent Swirling Pipe Flow with the Aid of Helicity Feb 2001

NIFS-681 Alexander A.Shishkin
Estafette of Drift Resonances, Stochasticity and Control of Particle Motion in a Toroidal Magnetic Trap, Feb 2001

NIFS-682 H Momota and G H. Miley,
Virtual Cathode in a Spherical Inertial Electrostatic Confinement Device, Feb 2001

NIFS-683 K Saito, R. Kumazawa, T Mutoh, T Seki, T Watari, Y Torii, D A Hartmann, Y Zhao A Fukuyama, F Shimpo, G. Nomura, M Yokota, M Sasao, M Isobe, M Osakabe, T Ozaki, K Narihara, Y Nagayama, S Inagaki, K Itoh, S Morita, A V Krasilnikov, K Ohkubo, M Sato, S Kubo, T Shimozuma, H Idei, Y Yoshimura, O Kaneko, Y Takeiri, Y Oka, K Tsumori, K Ikeda, A Komori, H Yamada, H Funaba, K Y Watanabe, S Sakakibara, M Shoji, R Sakamoto, J Miyazawa, K Tanaka, B J Peterson, N Ashikawa, S Murakami T Minami, S Ohakachi S Yamamoto, S Kado, H Sasao, H Suzuki, K Kawahata, P deVries, M Emoto, H Nakanishi, T Kobuchi N Inoue, N Ohyabu, Y Nakamura, S Masuzaki, S Muto, K Sato T Morisaki M Yokoyama, T Watanabe, M Goto, I Yamada, K Ida T Tokuzawa, , N Noda, S Yamaguchi, K Akaishi, A Sagara, K Toi, K Nishimura, K Yamazaki, S Sudo Y Hamada, O Motojima, M. Fujiwara,
Ion and Electron Heating in ICRF Heating Experiments on LHD Mar 2001

NIFS-684 S Kida and S Goto,
Line Statistics Stretching Rate of Passive Lines in Turbulence. Mar 2001

NIFS-685 R. Tanaka, T. Nakamura and T. Yabe,
Exactly Conservative Semi-Lagrangian Scheme (CIP-CSL) in One-Dimension Mar 2001